COMPUTER-AIDED DESIGN OF CIRCULARLY-POLARIZED CONFORMAL MICROSTRIP PATCH ANTENNA FOR TELEMETRY APPLICATIONS

Doris I. Wu and James Rieger

ABSTRACT

Planar microstrip antennas are desirable in many telemetry applications because they are small in size, light in weight, and conformal to most surfaces. The design and optimization of circularly-polarized omnidirectional microstrip arrays using a new software simulation tool are discussed in this paper. Critical design issues such as the optimization of each array element for circular polarization and the minimization of mutual couplings as well as feed network mismatch are examined. The software tool, which consists of a novel graphical user interface and a full-wave numerical simulator for a flat mounting surface, provides a testbed environment for the user to explore new designs as well as optimizing existing designs. Using this tool, the design of several wraparound arrays with different mounting cylinder radii are presented. Comparisons between measured and simulated data for two S-band 8-element wraparound arrays are also presented.

KEY WORDS

Microstrip Patch Antenna, Wraparound Array, Conformal Array, Circular Polarization, Computer-Aided Design Tool, Simulation, Modeling.

INTRODUCTION

Arbitrarily-oriented satellites and space vehicles such as missiles and rockets require an omnidirectional antenna to maintain a communication link with a central receiving unit. To avoid selective reception, a circularly-polarized (CP) omnidirectional antenna is often desirable. Previously-developed microstrip antennas for telemetry applications have primarily been linearly-polarized [1]. In designing a CP microstrip patch array, the design of each array element is crucial in yielding a good tradeoff between a low reflection loss and a low axial ratio. To yield a high gain, it is also important to minimize mismatch in the feed network. The analysis at the subarray level is often required to assess the effect of mutual coupling between patches. This paper examines the design of CP arrays at the element as well as the subarray level. We will

demonstrate how the design process can be enhanced by the use of a powerful computed-aided design (CAD) software tool for designing microstrip antennas [2,3].

ARRAY ELEMENT

The design of an array starts with the design of the element. The excitation of a CP element requires the simultaneous excitation of two orthogonal degenerate modes. Two commonly-used singly-fed CP elements are corners-truncated square patch and nearly-square patch. Figure 1 shows the geometry of the two types of CP element.

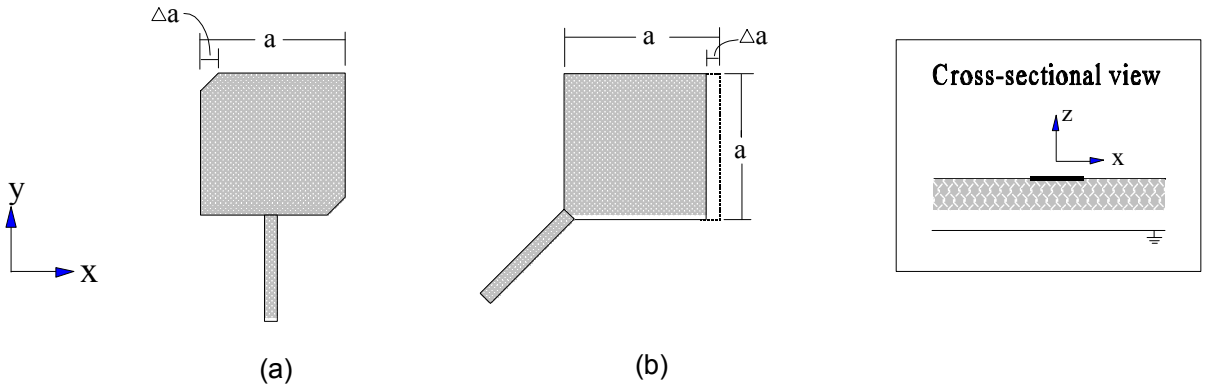

Figure 1: Circularly-polarized elements. (a) Corners-truncated. (b) Nearly-square.

The design of both types of element involves determining the patch dimension a and the truncated segment Δa. For a given substrate material, the designer must be able to adjust the truncated segment as well as the patch dimension to yield a minimum axial ratio at the desired operating frequency. While the designer can always optimize the patch by laboratory experimentation, this process can be laborious and time-consuming. For either type of element, the use of an accurate simulation tool becomes appealing in the design process. Figure 2 shows an example of the change in the axial ratio computed by our software tool for a corners-truncated square patch with different Δa. For the different cases shown in Figure 2, the substrate material is assumed to have a relative permittivity of 2.2 and a thickness of 1.58 mm. The dimension of the square patch is fixed at 43.29 mm. The overall change in Δa for the different cases shown in Figure 2 is less than 3.5 mm. However the minimum axial ratio corresponding to the different cases varies from 10 to 1.5 dB.

To assess the accuracy of the software tool, a nearly-square element with $a = 42.57$ mm and $\Delta a = 0.9$ mm was fabricated on a Duroid substrate ($\varepsilon_r = 2.2$ and thickness = 1.58 mm). The patch is tuned with an appropriate stub designed using the tool to match the input impedance of the patch to the 50 Ω feed line. Figure 3 shows a comparison of the measured return loss with the computed results. As can be seen, the

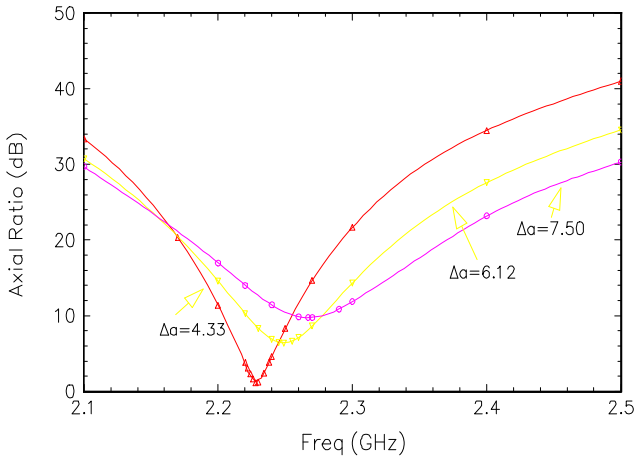

Figure 2: Axial ratio for a corners-truncated patch with different Δa.

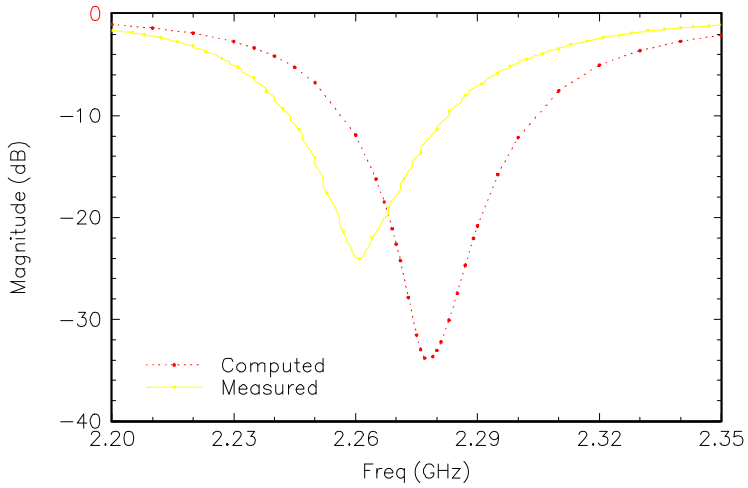

Figure 3: Measured and computed return loss for the nearly-square element.

predicted resonant frequency for this element is 2.28 GHz while the measured frequency is 2.26 GHz. The measured as well as the computed minimum axial ratio for this patch is approximately 1.3 dB at 2.28 GHz. The shift in the resonant frequency between the measured and computed data can be partially attributed to tolerances in the relative permittivity of the substrate. For a tolerance of up to $\pm 2\%$ in the relative permittivity, numerical experimentation shows that a $+2\%$ change can shift the computed resonant frequency shown in Figure 3 to 2.26 GHz while a -2% change can shift the resonant frequency to 2.30 GHz.

ARRAY DESIGN

The analysis of the antenna at the subarray level is also crucial in assessing mutual coupling effects. Because the simulation program of the CAD tool was developed using the full-wave, integral-equation approach [4], it takes into account all mutual couplings in the circuit. The effect of mutual coupling between the elements for different spacings

is assessed with the software tool. In particular, changes in the input impedance and axial ratio are examined for different element orientations and spacings. Figure 4 shows an example of the different orientations for the nearly-square element. Using our CAD tool, the response of the coupled patches is simulated for different separation distance between the patches. The results show that: 1). For patches with a separation distance of more than $\lambda_g/2$, where λ_g is the guided wavelength, the mutual coupling effect is negligible; 2). Mutual couplings have the most pronounced effect on the input impedance of the patch; 3). Mutual couplings increase the cross-polarization field component of the far-field pattern; and 4). The co-linear orientation shown in Figure 4(a) introduces more couplings than the rotated orientation shown in Figure 4(b).

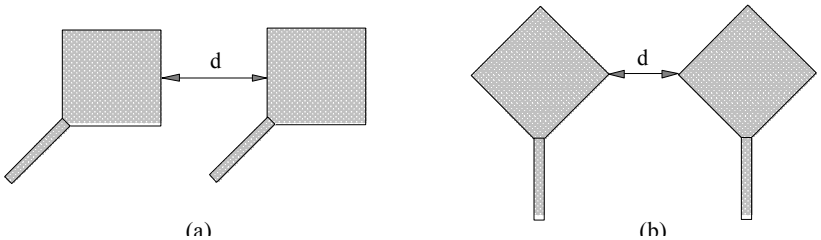

Figure 4: Two closely-spaced patches. (a) Co-linear orientation. (b) Rotated orientation.

With the dimensions of the element fixed, we proceed to the design of the subarray which entails devising a feed network for the proper feeding of each element. To achieve an omnidirectional pattern, each element of the array must be fed in equal magnitude and equal phase. To minimize mismatch, each power divider used in the feed network is modeled using the software tool. With the menu-driven graphical user interface, the geometry of the feed network as well as the array element can be created and adjusted easily. Figure 5 shows an 8-element corporate feed network designed using our tool. The entire feed network is simulated. The simulated results show that the return loss at the main feed point is less than -22 dB while the signals delivered to each element feed point are within 0.3 dB of one another in magnitude and 2 ^{o} in phase.

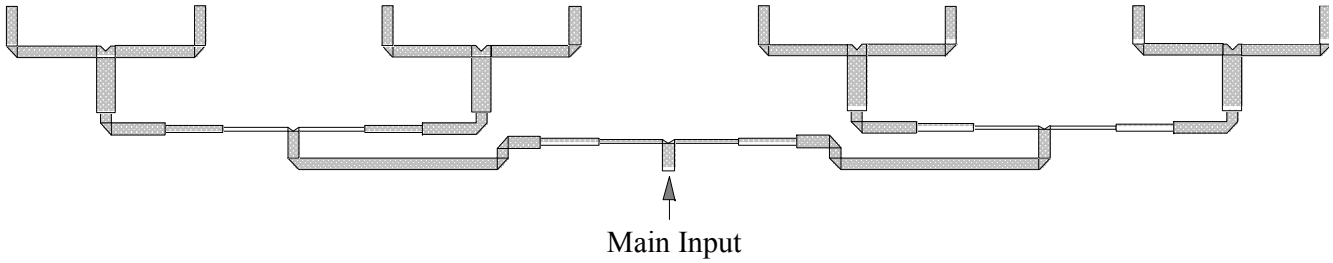

Figure 5: A corporate feed network for an 8-element array.

Since the current version of the CAD tool is for a flat mounting surface, we will consider only wraparound antennas with diameters that are not too small compared to a wavelength. To assess the rippling effect, a utility program was developed to compute the far-field patterns of an array consisting of identical patches equally spaced around an infinitely long cylinder. Figure 6 shows the generic configuration of the structure for computing the far-field patterns. In computing the far-field patterns, each patch is

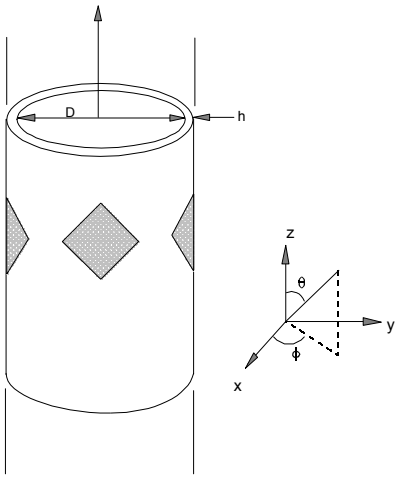

Figure 6: Patches on an infinitely long cylinder.

assumed to have identical current distribution and the current computed by our CAD tool for a single element is used as input. By simulating multiple elements together and using the resultant current on the element as the input, we can also assess the effect of mutual coupling between elements on the far-field patterns. This far-field computation program also allowed us to examine the change in the pattern ripples for different number of patches around the cylinder. Although sample designs were done for both 8" and 22"-diameter wraparound arrays, only the 8"-diameter examples are shown here.

Figures 7 and 8 show two 8-element arrays with corners-truncated and nearly-square elements, respectively. The dimensions of the feed network are adjusted for wrapping around an 8"-diameter cylinder. Each element has a tuning stub to match the input impedance to the input feed line. Similar to the feed network, the tuning stub for each element was designed using the CAD tool. The predicted resonant frequency for both arrays is 2.28 GHz. The minimum ripple in the roll plane computed for both arrays is less than 2 dB. However, because the computation of the far-field does not take into account the feed network, the actual ripple level is expected to be higher.

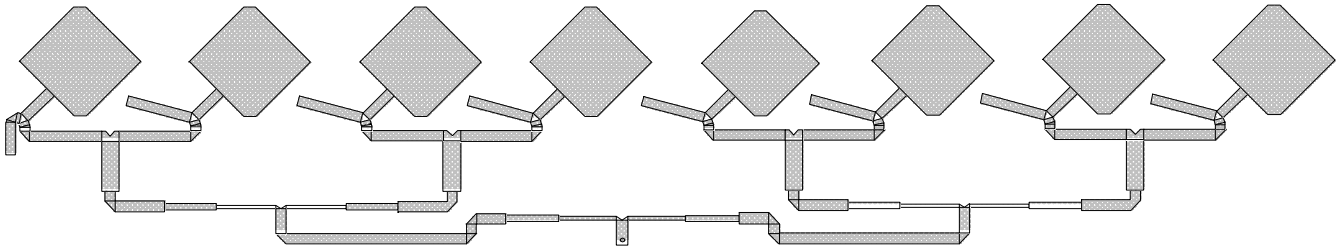

Figure 7: An 8-element array with corners-truncated elements.

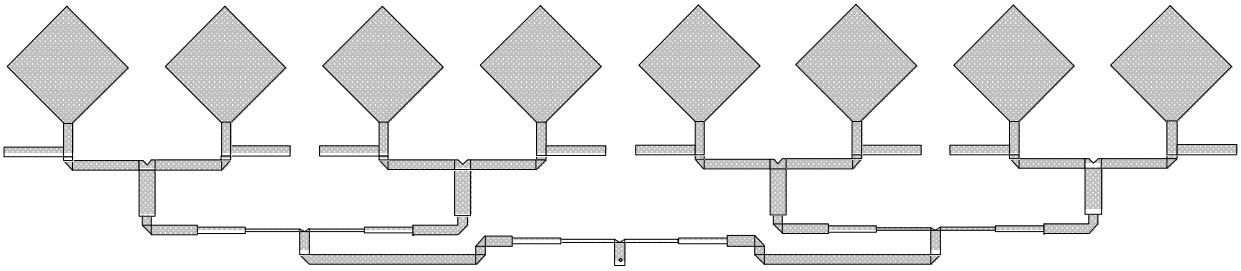

Figure 8: An 8-element array with nearly-square elements.

To assess the effectiveness of the CAD tool, the arrays shown in Figures 7 and 8 were fabricated on non-woven substrates and rolled into 8" wraparounds. Although the substrates used for both arrays had the same dielectric constant and thickness, they were supplied by different manufacturers. Figures 9 and 10 show the Smith chart plotting of the measured return loss for the corners-truncated and the nearly-square wraparounds, respectively. The measured resonant frequencies for the corners-truncated and the nearly-square wraparounds are 2.27 GHz and 2.33 GHz, respectively. The difference in the resonant frequency between the two wraparounds could be attributed to variation in the substrates from different manufacturers. Figure 11 shows the preliminary measurement on the far-field pattern of the main component over half of the roll plane at $\theta = 90^{o}$ for both wraparounds. As can be seen, the ripples in the measured pattern for the corners-truncated and the nearly-square wraparounds are 5 dB and 3 dB, respectively. These ripple levels are higher than the computed values as expected. Additional testings to assess the performance of these wraparound arrays will be conducted.

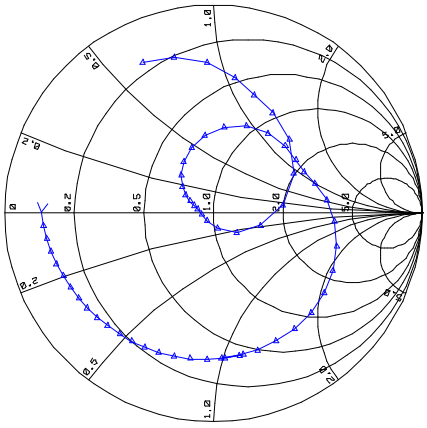

Figure 9: Measured return loss for the corners-truncated wraparound array.

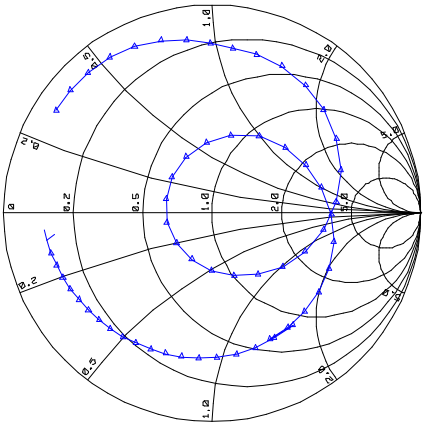

Figure 10: Measured return loss for the nearly-square wraparound array.

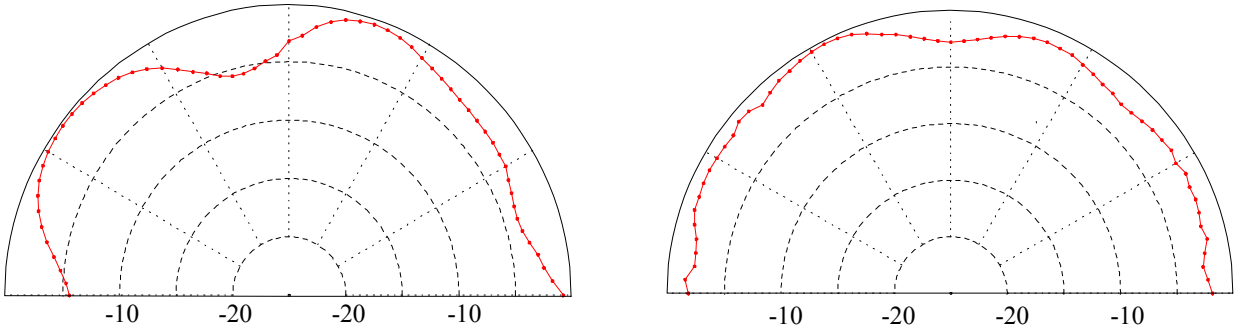

(a) (b)

Figure 11: Measured radiation pattern in the $2 = 90^{o}$ roll plane. (a) Corner-truncated wraparound. (b) Nearly-square wraparound.

CONCLUSIONS

The design of omnidirectional circularly-polarized wraparound arrays using a computer-aided design tool has been discussed. The availability of the software tool for designing microstrip antennas at the element as well as the feed network level clearly enhanced our design process. Although the current version of the tool does not take curvature into account in the design process, for large mounting cylinders, the effect is minimal. Work is currently underway to develop a set of CAD tools for designing wraparound arrays which will take curvature into account for small mounting cylinders.

REFERENCES

1. Munson, R. E., "Conformal microstrip antennas and microstrip phased arrays," IEEE. Trans. on Antennas and Prop. , vol. 22, pp. 74-78, Jan. 1974.

2. Wu, D. I., Ensemble User's Guide. Boulder Microwave Technologies, Inc., Dec., 1993.

3. Wu, D. I. and L. D. DiDomenico, "Design of dual-linear microstrip array elements," IEEE Antennas and Propagation Intern. Symposium Proceedings , p. 1208-1211, June, 1993.

4. Wu, D. I. and Chang, D. C., "A review on the electromagnetic properties and full-wave analysis of the guiding structures in MMICs," Invited paper, Proceedings of IEEE, pp. 1529-1537, Oct. 1991.